ACSNANO

www.acsnano.org

ARTICLE

Gold Chain Formation via Local Lifting of Surface Reconstruction by Hot Electron Injection on H_2 (D_2)/Au(111)

P. Merino,* A. Rosławska, A. Grewal, C. C. Leon, C. Gonzalez, K. Kuhnke, and K. Kern

Cite This: https://dx.doi.org/10.1021/acsnano.0c05507

Read Online

ACCESS | Metrics & More | Article Recommendations | Supporting Information

ABSTRACT: The hexagonal close packed surface of gold shows a 22 × $\sqrt{3}$ "herringbone" surface reconstruction which makes it unique among the (111) surfaces of all metals. This long-range energetically favored dislocation pattern appears in response to the strong tensile stress that would be present on the unreconstructed surface. Adsorption of molecular and atomic species can be used to tune this surface stress and lift the herringbone reconstruction. Here we show that herringbone reconstruction can be controllably lifted in ultrahigh vacuum at cryogenic temperatures by precise hot electron injection in the presence of hydrogen molecules. We use the sharp tip of a scanning tunneling microscope (STM) for charge carrier injection and characterization of the resulting chain nanostructures. By comparing STM images, rotational spectromicroscopy and *ab initio* calculations, we show that formation of gold atomic chains is associated with release of gold atoms from the surface, lifting of the reconstruction, dissociation of H_2 molecules, and formation of surface hydrides. Gold hydrides grow in a zipper-like mechanism forming chains along the [1$\bar{1}$0] directions of the Au(111) surface and can be manipulated by further electron injection. Finally, we demonstrate that Au(111) terraces can be transformed with nearly perfect terrace selectivity over distances of hundreds of nanometers.

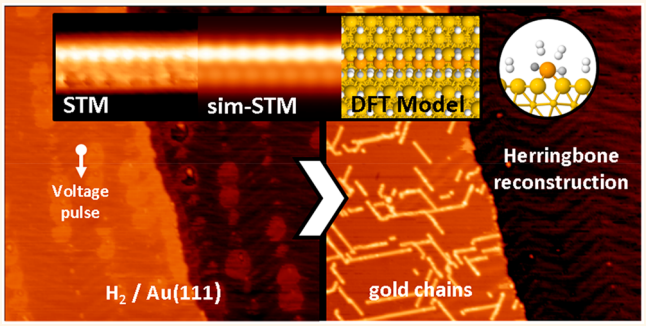

KEYWORDS: *herringbone reconstruction, gold chain, molecular hydrogen, gold hydride, STM*

The 22 × $\sqrt{3}$ herringbone reconstruction of Au (111) consists of a tensile stress-induced periodic arrangement that leads to a dislocation pattern separating regions of fcc and hcp stacking. The stacking domains are separated by soliton walls which form a secondary structure resulting in partial dislocation elbow sites which imprint the characteristic "herringbone" aspect of the surface.[1] In the top layer, 23 atoms are laterally compressed to fit into a length corresponding to 22 atoms from the bulk along the [0$\bar{1}$1] direction.[2] By inducing this reconstruction the Au(111) surface relaxes its intrinsic tensile stress by 22%.[3] Other mechanisms for releasing this stress have been found at gold interfaces permitting nanoscale surface engineering.[4] "Magic gold fingers", one atom layer in height, can be formed on the (111) surface of gold via nanomanipulations driven by localized electric field with a scanning tunneling microscope (STM).[2,5] Relaxations of the herringbone reconstruction are also observed in electrochemistry experiments.[6] When reactive species such as chlorine[7] or sulfur[8] are deposited on Au(111) in ultrahigh vacuum condition (UHV) they promote the formation of adatom−adsorbate complexes that lift the reconstruction.[9,10] Alkali metals deposited on Au(111) also distort the periodicity of the reconstruction by influencing the elastic stress of the topmost layer.[11] Other adsorbed species such as O atoms, iron phthalocyanine or perylene, induce partial lifting of the 22 × $\sqrt{3}$ reconstruction due to anisotropic surface stress induced by interfacial charge transfer.[12,13] Hydrogen (H_2) and its isotope deuterium (D_2) have been investigated at the atomic-scale adsorbed on Au(111) but no effect on the herringbone reconstruction has been reported to date.[14−16] Hydrogen molecules physisorb and develop into coverage dependent superstructures. At low concentrations they form a surface-state mediated Fermi superlattice,[17] while at coverages close to one monolayer they aggregate into close

Received: July 3, 2020
Accepted: October 20, 2020

ACS Publications © XXXX American Chemical Society

https://dx.doi.org/10.1021/acsnano.0c05507
ACS Nano XXXX, XXX, XXX−XXX

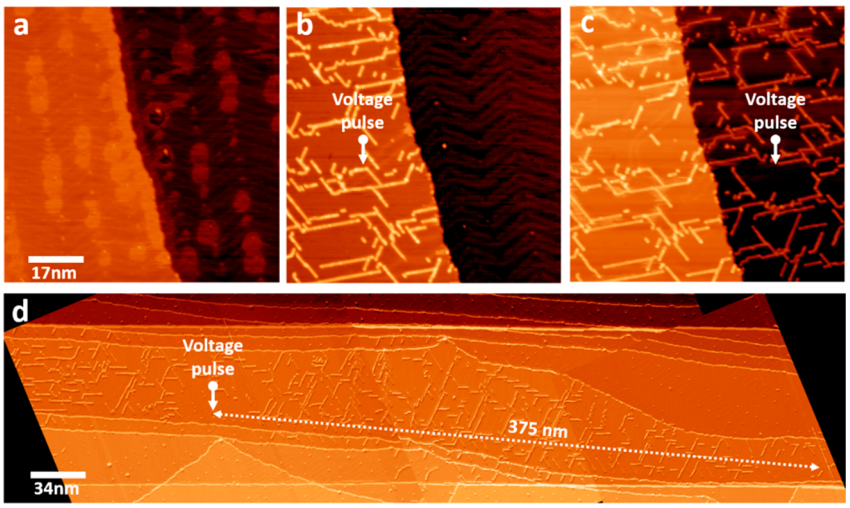

Figure 1. Mesoscopic extension and terrace selectivity of the chain formation. (a)−(c). STM images showing the formation of chains on the Au(111) surface and lifting of the herringbone reconstruction. Single voltage pulses were applied at the indicated positions, a first pulse on the left-hand side (upper terrace) between images (a) and (b) and a second pulse on the right-hand side (lower terrace) between images (b) and (c). Size: 85 × 85 nm^2, 100 pA. a) + 20 mV, b) and c) + 2.7 V. (d). The long-range of the chain-creation process is demonstrated by the extended topography merged together from three individual 200 × 200 nm^2 images.

packed two-dimensional clusters,[18,19] in all cases leaving the surface herringbone reconstruction intact.

The interaction between hydrogen and gold atoms has been predicted to be strong but dissociating H_2 molecules normally needs activation on a catalyzer.[20] Gold is renowned as the noblest of all metals;[21] yet, gold nanostructures can show high catalytic activity for many reduction and oxidation reactions,[22−24] and in particular for dihydrogen dissociation.[25−27] Important size effects have been observed leading to the conclusion that the edges and corners of the nanostructures are the active sites for dissociation.[28,29] For this reason, flat gold surfaces are considered to be chemically inert for bond dissociation, as they present a low amount of undercoordinated atoms.[30] Engineering routes that increase the number of edge or corner atoms per unit area on Au(111) would boost the catalytic activity of the otherwise inert surface for the study of hydrogenation reactions.

Here, we show that the herringbone reconstruction can be locally lifted on individual terraces by applying voltage pulses with the tip of a scanning tunneling microscope (STM) in the presence of physisorbed H_2 and D_2 molecules. By injecting hot electrons, the "23rd extra atom" of each unit cell gets promoted from the top layer onto the terrace and stabilizes the formation of Au monatomic chains along the [1$\bar{1}$0] directions of the Au(111) surface. We rationalize these experimental findings with extensive ab initio calculations and STM simulations, confirming that upon Au adatom lifting, hydrogen molecules spontaneously dissociate and covalently bond with Au to form interfacial gold hydrides that trigger chain formation in a zipper-like mechanism.

RESULTS AND DISCUSSION

Figure 1a−c show a sequence of three STM images illustrating the chain generation process. Two Au(111) terraces are present on the left and right-hand sides of the images separated by a monatomic step. Figure 1a shows the surface prior to application of voltage pulses. Hydrogen physisorbed on the terraces forms disk-shaped islands decorating the elbows of the herringbone reconstruction (Figure 1a).[1,18,19] The arrow in Figure 1b marks the position in the left terrace where we applied a +10 V voltage pulse for 100 ms (with positive polarity implying the injection of electrons from the tip to the surface). After the first pulse, the herringbone reconstruction is lifted and one-dimensional nanostructures cover the terrace where the voltage pulse was applied. The structures preferentially align with the three high-symmetry directions, equivalent to the [1$\bar{1}$0] direction of the Au(111) surface. In a second step, another voltage pulse was applied on the right-hand-side terrace transforming the second, still herringbone reconstructed terrace in the same way as described before (see Figure 1c). The chain generation process is limited to one terrace but extends over large distances. A voltage pulse under tunneling conditions promotes transient injection of hot electrons (i.e., electrons with energies hundreds of times greater than the available thermal energy).[31] The strict terrace selectivity suggests that the observed transformation process is mediated by the electron surface state,[32] although other mechanisms involving charge transport on the surface, such as propagation of surface plasmon polaritons, may also play a role.

Inspecting the range of transformation, we find that a single pulse can generate chains more than 350 nm away from the position where the pulse was applied (Figure 1d). The chains are straight and can be very long (>20 nm) but encounters with other chains limit their growth. We observe that the chain formation probability saturates at 100% for pulses of 100 ms duration and +7 V bias (see Figure S5 in the Supporting Information (SI)). Chains can also be produced at lower bias voltages but with lower efficiency. Regardless of how chains are made, once they have formed, their shape can be modified with further pulsing (see SI Figure S6). Evaluation of their structure indicates that the number of chain atoms is approximately one adatom per 22 top layer atoms for sufficiently strong pulses, which suggests that the chains consist exclusively of Au atoms expelled from the interface upon lifting the herringbone reconstruction (see SI Figure S1). For milder pulses, both chains and a residual herringbone reconstruction can coexist on the same terrace.

https://dx.doi.org/10.1021/acsnano.0c05507
ACS Nano XXXX, XXX, XXX−XXX

In Figure 2 we present high-resolution images of a short individual chain formed by a voltage pulse on a surface covered

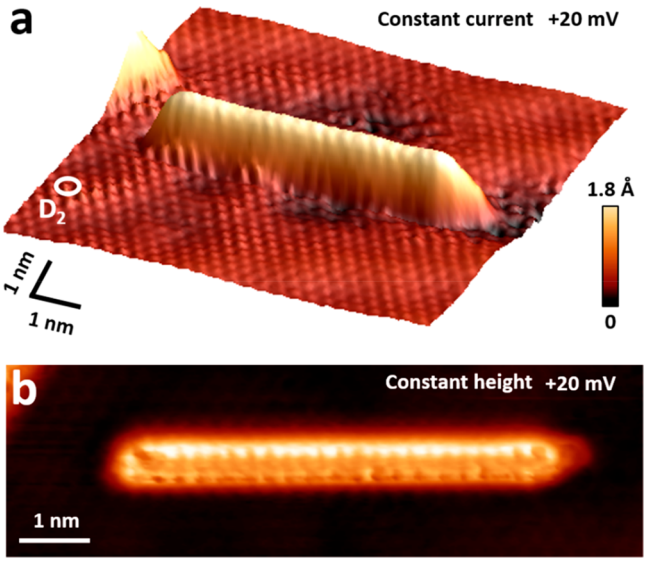

Figure 2. High-resolution images of a short chain. (a) Three-dimensional topographic STM image of a characteristic atomic chain. Individual D_2 molecules covering the whole area in a dense phase are resolved on the surface (one molecule is marked within a white ellipse) as a hexagonal pattern and on the chain. Nine ×9 nm^2, 30 pA, +20 mV. (b) Constant height current map of a quasi-1D chain measured showing atomic resolution. Every protrusion on the chain can be ascribed to a single D_2 molecule, 9 × 3 nm^2, +20 mV.

by isotopic hydrogen molecules (deuterium D_2) injected into the chamber to replace the residual H_2 gas. Figure 2a shows a pseudo 3D representation of a constant current measurement obtained at a bias voltage of +20 mV. The chain is 6.5 nm long and has an apparent height of 1.55 Å. Individual atomic-scale protrusions are resolved on top of the chain. The features are better resolved in the constant height STM image presented in Figure 2b, which reveals that the chain consists of two rows of atomic-scale features where one appears higher than the other. At +20 mV the molecules exhibit a high density of states and enhanced conductivity characteristic of physisorption. Therefore, the protrusions can be attributed to individual D_2 molecules physisorbed on the chain rather than being chemisorbed to Au atoms. Indeed, a close packed layer of D_2 molecules can be resolved as a 2D mantle covering the terrace (one molecule is marked in Figure 2a).

To gain further insight we perform local tunneling spectroscopy on the chains. Figure 3a shows a dI/dV spectrum of D_2/Au(111) featuring the surface state of Au(111) at −0.5 eV and the vibrational peak structure around the Fermi level characteristic for D_2 on gold surfaces.[33,34] The electronic states between −40 mV and +40 mV and the two negative differential conductance peaks correspond to the opening of rotational and vibrational channels in inelastic tunneling. The energy and relative intensity of the vibrational peaks is very sensitive to the, isotopic species, the nanocavity size and the exact adsorption configuration of the molecules on the surface.[33,34] Figure 3c shows a constant height dI/dV map at V_{bias}= +20 mV. The presence of D_2 molecules covering the chain can be deduced from the high intensity of the D_2-related state measured on top of it. In addition, individual D_2

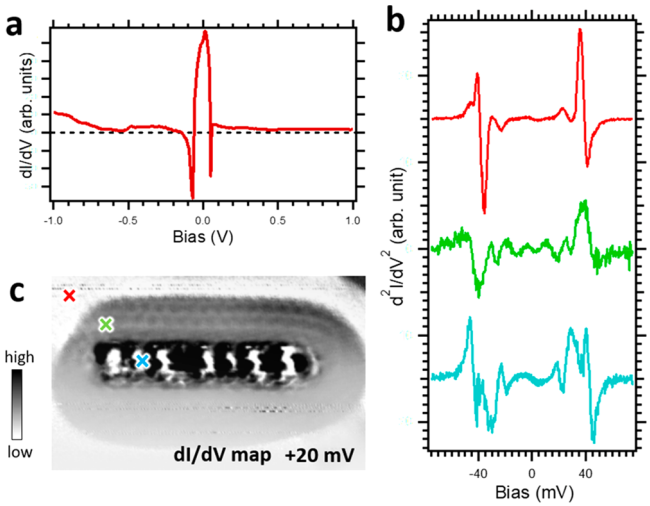

Figure 3. Spectromicroscopy characterization of a short chain generated using D_2 (a) Wide range (−1 V to +1 V) dI/dV spectrum of the D_2/Au(111) system. (b) Inelastic tunneling electron spectroscopy as measured by d^2I/dV^2 of the D_2/Au(111) chains. The positions where the individual spectra were measured are marked by color-coded crosses in panel c. The intensity of the red curve was divided by a factor of 4. (c) Chain mapped under constant height dI/dV condition at +20 mV using a functionalized tip. The chain is surrounded by an oblong island of dense D_2 molecules, the structure of which can be resolved near the upper edge in the image, size: 6.9 × 3.8 nm^2.

molecules are resolved surrounding the atomic chain forming an oblong island.[18,19] In Figure 3b we present d^2I/dV^2 spectra obtained on the positions marked in Figure 3c. Strikingly, the d^2I/dV^2 spectrum obtained on the region free of D_2 molecules (red color) shows sharp peaks at ±40 meV with 5 meV width which is a strong indication of tip functionalization with a picked-up molecule. Functionalization enhances contrast and lateral resolution.[14,15,35−37] In addition, the molecule at the tip increases the sensitivity to the local environment and the spatial variations of the potential energy of the surface which permits one to perform, so-called, rotational spectro-microscopy maps.[16] Accordingly, Figure 3c charts the interaction between deuterium on the tip and on the sample. The d^2I/dV^2 spectrum recorded on the dense D_2 island (green curve) shows broader (10 meV) peaks and twice the number of features, indicative of vibrational coupling between the molecule at the tip and those on the surface.[38,39] The d^2I/dV^2 spectrum recorded on top of the chain (blue curve) also exhibits twice as many peaks and dip features, some of them being broad (10 meV) and some being sharp (5 meV). These observations indicate that D_2 molecules on top of the chain interact less strongly with D_2 at the tip than the molecules in the densely packed island surrounding the chain.

In Figure 4a we present the ball-and-stick model of the energetically most stable structure determined by our density functional theory (DFT) simulations. It consists of a concatenation of gold adatoms covalently bonded with two hydrogen atoms at the sides of the chain. One of the two hydrogen atoms bonds exclusively to the adatom (depicted in dark gray in Figure 4a) and the other bridges between the adatom and a Au atom on the surface (depicted in light gray). The whole structure is fully covered with a monolayer of vertically aligned physisorbed H_2 molecules responsible for the atomic-scale features resolved in the STM images and dI/dV

https://dx.doi.org/10.1021/acsnano.0c05507
ACS Nano XXXX, XXX, XXX−XXX

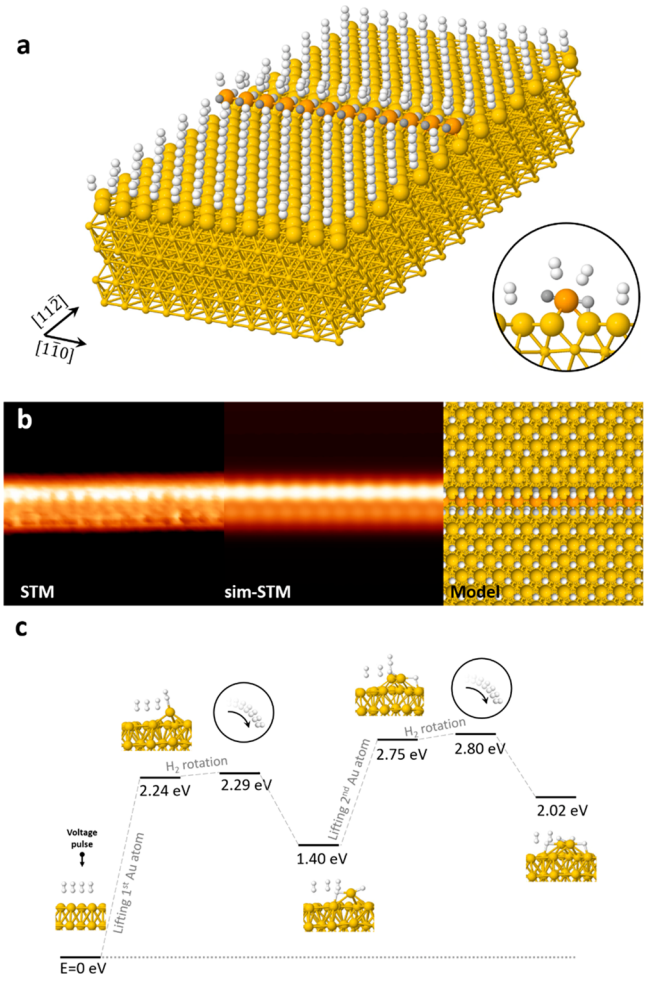

Figure 4. Theoretical structural model, STM simulation and mechanism for chain formation. (a) Ball-and-stick model of the lowest energy structure. Yellow and white balls correspond to gold and hydrogen atoms, respectively. The orange balls represent the Au atoms forming chains aligned with the[1$\bar{1}$0] directions of the Au(111) surface. Light and dark gray balls represent H atoms originating from a dissociated molecule. Inset: Side view of the ball-and-stick model of the best fit structure. The vertically aligned hydrogen molecules cover the surface and the hydrogen atoms are asymmetrically bound to the Au chain. (b) Constant height STM image (left-hand side) of an atomic chain, constant height STM simulation (middle), and top view of the ball-and-stick structure (right-hand side). The maxima in the simulation correspond to the positions of the hydrogen molecules physisorbed on the chain. (c) Schematic representation of the initial steps involved in the chain formation from DFT calculations: Au-lifting, H_2 rotation, Au-induced hydrogen dissociation, next-neighbor Au lifting. The diagram associated with the lowest barrier reaction pathway reveals a mechanism involving the energy barriers that have to be overcome by the energy provided by the injected hot electrons.

maps. In Figure 4b we present a comparison between the STM simulation of the structure and the experimental images. On the left-hand side is the measurement, in the middle the STM simulation, and on the right-hand side the top view of the ball-and-stick model. The agreement between experimental and simulated STM images is very good. The H_2 molecules physisorbed over the chain form the characteristic zigzag pattern observed in the experimental STM image. The two rows of H_2 molecules are physisorbed at different heights over the chains, due to the asymmetric Au−H bonding configuration. The height difference is resolved in the STM image simulation, as one of the rows appears brighter than the other thus reproducing the small asymmetry observed in the chain topography.

Ab initio calculations permit us to determine the formation mechanism of the atomic chains. We start our analysis by reproducing the herringbone reconstruction building a slab with the $(22 \times \sqrt{3})$ periodicity including six layers of Au atoms in the unit cell (see the Supporting Information for details).[40] In our calculations, when the "extra 23rd atom" of the herringbone reconstruction is placed as an adatom on a pristine Au(111) unreconstructed surface, it returns back to the top bulk layer upon relaxation of the system confirming that theory reproduces the fact that the herringbone reconstruction is energetically favorable.

We have simulated and evaluated the chain formation by dividing the process in steps. In Figure 4c we present a scheme showing the energy of the initial intermediate states. In a first step, we start pulling up one of two "extra 23rd atoms" from the $22 \times \sqrt{3}$ unit cell with an energy cost of 2.24 eV. The calculations have been made with a doubled $22 \times \sqrt{3}$ unit cell, that is, $22 \times 2\sqrt{3}$, which leaves the other three "extra 23rd atoms" embedded in the surface. The following step considers the rotation of one H_2 molecule from its original orientation (perpendicular to the surface) to a parallel position on the lifted atom. This process increases the energy of the system by 0.05 eV. When a hydrogen molecule is physisorbed parallel to the surface on top of the gold adatom, the highly undercoordinated gold adatom catalyzes its exothermic dissociation forming a stable interfacial Au-hydride chemisorbed complex. The system further relaxes by migrating one of the hydrogen atoms in a bridge position between the adatom and the nearest neighboring Au atom located in the surface. The total energy gain by the system upon H_2 dissociation and hydride formation is −0.89 eV.

In a second step, another Au atom is promoted to the interface. It will preferably be the next atom in [1$\bar{1}$0] direction neighboring the first formed hydride (see SI Figure S9 in the Supporting Information). This newly expelled atom is released from the next row of compressed atoms in the surface reconstruction. The total energy cost of this process is 1.35 eV. Since these 1.35 eV for pulling out a second gold adatom are 0.89 eV lower than the 2.24 eV required to lift the first atom, the system will tend to form atomic chains in a coordinated zipper-like fashion rather than expelling atoms at separated locations. After rotating the H_2 on top, the second adatom spontaneously dissociates the molecule and forms a second gold hydride complex with an energy gain of −0.78 eV. We speculate that the hot electrons injected by the voltage pulse excite out-of-plane phonon modes that help to pull Au atoms above the surface plane. The dissociation of the very first H_2 molecule by the undercoordinated Au adatom results in nucleating a chain that leads to continued lifting of neighboring atoms in a zipper-like fashion. This process in turn leads to quasi-1D chains observed in the experiment. Surface diffusion simulations further corroborate the zipper-like chain growth mechanism, as the formation of 2D clusters would be favored over nm-long linear chains when we assume nucleation from randomly generated gold hydride monomer and on-surface diffusion (see Supporting Information).

The final $22 \times 2\sqrt{3}$ structure with all four Au "extra 23rd atoms" following the [1$\bar{1}$0] direction promoted as adatoms, the

https://dx.doi.org/10.1021/acsnano.0c05507
ACS Nano XXXX, XXX, XXX−XXX

four H_2 molecules dissociated, the herringbone reconstruction lifted and the development of a (1×1) Au(111) surface has a total energy 3.76 eV higher than the initial structure. Given the large energy barriers involved in the adatom lifting process, we propose that the injection of hot electrons helps the system surmount these barriers and reach a local energy minimum which is stabilized at the cryogenic temperatures of the experiment. Indeed, gold nanowires are known to dissociate hydrogen molecules with very low activation barriers.[20,29,41,42] Note that in order to simplify the calculations we have used only four H_2 adsorbate molecules in the simulation of the growth process. We estimate that the effect of the full hydrogen monolayer mantle covering the surface is negligible in our analysis of the energetics of the system.

CONCLUSIONS

To conclude, we present a combined experimental and theoretical atomic-scale study that demonstrates the controlled generation of atomic chains on the Au(111) surface upon hot electron injection with voltage pulses. The mechanism involves the expulsion of the "23rd extra atom" of the herringbone reconstruction to the surface followed by stabilization in the presence of hydrogen (deuterium) molecules. This process lifts the herringbone reconstruction and forms one-dimensional chains in a terrace selective manner over mesoscopic distances. Combining experiments with *ab initio* calculations we determine that the chains are aligned with the three equivalent $[1\bar{1}0]$ directions and consist of Au adatoms stabilized by H atoms. Hydrogen molecules spontaneously dissociate in the presence of undercoordinated Au atoms and form chemical bonds with them. The resulting gold hydrides remain stabilized on the surface and further ease the promotion of a first-neighbor Au atom to the interface, fostering the formation of the chains in a zipper-like fashion. Finally, the hydride adatom chains are covered with the excess molecules which form a mantle of vertically aligned H_2 (D_2) and determine the atomic scale periodic structure observed in the STM images. Our finding enables locally functionalizing Au(111) surfaces that may enhance their catalytic activity for hydrogen dissociation and permit the study of hydrogenation chemical reactions at the atomic-scale in a model system.

METHODS/EXPERIMENTAL

Sample Preparation. Au(111) single crystal samples were cleaned by repeated cycles of Ar^+-sputtering and annealing which result in a clean surface with terraces of 10−100 nm width showing the herringbone reconstruction everywhere on the surface as confirmed with STM. Clean Au(111) at ∼10 K is exposed to a partial pressure of D_2 of 1.5×10^{-7} mbar (Linde Minican 99% purity) for 2 h with no line of sight between the leak valve and the sample. Due to this fact and the geometry of the vacuum chamber the adsorbates start to appear on the surface only after several hours of dosing D_2.[15] Alternatively, H_2 from residual background gas ($\sim 10^{-11}$ partial pressure), as confirmed by a detailed residual gas analysis, present in the UHV cryostat is condensed on the Au(111) surface and used in the experiments.

STM Measurements. The experiments were conducted in a home-built low-temperature (4.2 K) STM, under ultrahigh vacuum conditions. The dI/dV spectra were obtained using a lock-in amplifier, with a modulation voltage of V_{rms} = 10 mV at 938.5 Hz. Analysis of STM and STS data were performed with the software WSxM.[43] d^2I/dV^2 spectra were measured by analyzing the second harmonic of the excitation frequency.

Theoretical Details. DFT calculations have been performed using the FIREBALL package (see the Supporting Information for details).[44] We create a herringbone unit cell with a $22 \times \sqrt{3}$ periodicity including six slabs of Au atoms (266 gold atoms). This unit cell has been doubled for the energetic calculations (532 Au atoms plus four H_2 molecules). Due to the large lattice vectors, the Brillouin zone (BZ) has been sampled only with the gamma point. The extracted atoms were moved up in steps of 0.25 Å until the required final height is found. In such processes, the Z-coordinate of the uppermost Au atoms remains fixed. Using this geometry as a starting point, the H_2 molecule is rotated and finally it spontaneously dissociates. Following the preferential directions observed in the experiment, the geometry of the final structure should in fact be simulated by using a slightly different $22 \times 2\sqrt{3}$ periodicity with the exact same size and number of atoms. In the search of the most stable structure, we have tried 16 distinct initial atomic configurations. In a final step, we fully cover the Au surface and the Au−H chain with H_2 molecules, resulting in a structure of 716 atoms. For the STM simulations, we used a homemade package based on the Keldysh-Green function formalism.[45]

ASSOCIATED CONTENT

Supporting Information

The Supporting Information is available free of charge at https://pubs.acs.org/doi/10.1021/acsnano.0c05507.

Au chain adatom density; Chain length statistics; Chain morphology; Diffusion simulations; Chain formation efficiency as a function of voltage and current of the pulses; Modification of the chains with consecutive voltage pulses; Supplementary theory and Supplementary references (PDF)

AUTHOR INFORMATION

Corresponding Author

P. Merino − *Max Planck Institute for Solid State Research, D70569 Stuttgart, Germany; Instituto de Ciencia de Materiales de Madrid, CSIC, E28049 Madrid, Spain; Instituto de Física Fundamental, CSIC, E28006 Madrid, Spain;* orcid.org/0000-0002-0267-4020; Email: pablo.merino@csic.es

Authors

A. Rosławska − *Max Planck Institute for Solid State Research, D70569 Stuttgart, Germany;* orcid.org/0000-0002-0317-1775

A. Grewal − *Max Planck Institute for Solid State Research, D70569 Stuttgart, Germany*

C. C. Leon − *Max Planck Institute for Solid State Research, D70569 Stuttgart, Germany;* orcid.org/0000-0003-4132-4645

C. Gonzalez − *Departamento de Física Teórica de la Materia Condensada and Condensed Matter Physics Center (IFIMAC), Facultad de Ciencias, Universidad Autónoma de Madrid, E28049 Madrid, Spain; Departamento de Física de Materiales, Universidad Complutense de Madrid, 28040 Madrid, Spain; Instituto de Magnetismo Aplicado UCM-ADIF, E-28232 Las Rozas de Madrid, Spain*

K. Kuhnke − *Max Planck Institute for Solid State Research, D70569 Stuttgart, Germany;* orcid.org/0000-0001-9981-1732

K. Kern − *Max Planck Institute for Solid State Research, D70569 Stuttgart, Germany; Institut de Physique, École Polytechnique Fédérale de Lausanne, 1015 Lausanne, Switzerland*

Complete contact information is available at: https://pubs.acs.org/10.1021/acsnano.0c05507

https://dx.doi.org/10.1021/acsnano.0c05507
ACS Nano XXXX, XXX, XXX−XXX

Notes

The authors declare no competing financial interest.

ACKNOWLEDGMENTS

C.G. was funded by Spanish Ministry of Science, Innovation and Universities under the projects MAT2017-88258-R and MDM-2014-0377 (María de Maeztu Programme for Units of Excellence in R&D). C.G. acknowledge the computer resources at Cibeles and the technical support provided by the Scientific Computing Center at UAM, project FI-2019-0028. PM acknowledges support from the A.v. Humboldt Foundation, the ERC Synergy Program (grant no. ERC-2013-SYG-610256, Nanocosmos), Spanish MINECO (MAT2017-85089-C2-1-R) and the "Comunidad de Madrid" for its support to the FotoArt-CM Project S2018/NMT-4367 through the Program of R&D activities between research groups in Technologies 2013, cofinanced by European Structural Funds.

REFERENCES

(1) Barth, J. V.; Brune, H.; Ertl, G.; Behm, R. J. Scanning Tunneling Microscopy Observations on the Reconstructed Au(111) Surface: Atomic Structure, Long-Range Superstructure, Rotational Domains, and Surface Defects. *Phys. Rev. B: Condens. Matter Mater. Phys.* **1990**, *42*, 9307−9318.

(2) Guo, Q.; Yin, F.; Palmer, R. E. Beyond the Herringbone Reconstruction: Magic Gold Fingers. *Small* **2005**, *1*, 76−79.

(3) Bach, C. E.; Giesen, M.; Ibach, H.; Einstein, T. L. Stress Relief in Reconstruction. *Phys. Rev. Lett.* **1997**, *78*, 4225−4228.

(4) Hasegawa, Y.; Avouris, P. Manipulation of the Reconstruction of the Au(111) Surface with the STM. *Science* **1992**, *258*, 1763−1765.

(5) Yin, F.; Palmer, R.; Guo, Q. Nanoscale Surface Recrystallization Driven by Localized Electric Field. *Phys. Rev. B: Condens. Matter Mater. Phys.* **2006**, *73*, 73405.

(6) Wu, Q.; Shang, W. H.; Yan, J. W.; Xie, Z. X.; Mao, B. W. Metal Adlayer-Induced Relaxation of Au(111) Reconstruction under Electrochemical Control. *J. Phys. Chem. B* **2003**, *107*, 4065−4069.

(7) Andryushechkin, B. V.; Cherkez, V. V.; Gladchenko, E. V.; Pavlova, T. V.; Zhidomirov, G. M.; Kierren, B.; Didiot, C.; Fagot-Revurat, Y.; Malterre, D.; Eltsov, K. N. Self-Organization of Gold Chloride Molecules on Au(111) Surface. *J. Phys. Chem. C* **2013**, *117*, 24948.

(8) Maksymovych, P.; Sorescu, D. C.; Yates, J. T. Gold-Adatom-Mediated Bonding in Self-Assembled Short-Chain Alkanethiolate Species on the Au(111) Surface. *Phys. Rev. Lett.* **2006**, *97*, 146103.

(9) Maksymovych, P.; Voznyy, O.; Dougherty, D. B.; Sorescu, D. C.; Yates, J. T. Gold Adatom as a Key Structural Component in Self-Assembled Monolayers of Organosulfur Molecules on Au(111). *Prog. Surf. Sci.* **2010**, *85*, 206−240.

(10) Cossaro, A.; Mazzarello, R.; Rousseau, R.; Casalis, L.; Verdini, A.; Kohlmeyer, A.; Floreano, L.; Scandolo, S.; Morgante, A.; Klein, M. L.; Scoles, G. X-Ray Diffraction and Computation Yield the Structure of Alkanethiols on Gold(111). *Science* **2008**, *321*, 943−946.

(11) Barth, J. V.; Behm, R. J.; Ertl, G. Mesoscopic Structural Transformations of the Au(111) Surface Induced by Alkali Metal Adsorption. *Surf. Sci.* **1994**, *302*, L319−L324.

(12) Sun, J. T.; Gao, L.; He, X. B.; Cheng, Z. H.; Deng, Z. T.; Lin, X.; Hu, H.; Du, S. X.; Liu, F.; Gao, H.-J. Surface Reconstruction Transition of Metals Induced by Molecular Adsorption. *Phys. Rev. B: Condens. Matter Mater. Phys.* **2011**, *83*, 115419.

(13) Min, B. K.; Deng, X.; Pinnaduwage, D.; Schalek, R.; Friend, C. M. Oxygen-Induced Restructuring with Release of Gold Atoms from Au(111). *Phys. Rev. B: Condens. Matter Mater. Phys.* **2005**, *72*,. DOI: 10.1103/PhysRevB.72.121410

(14) Weiss, C.; Wagner, C.; Temirov, R.; Tautz, F. S. Direct Imaging of Intermolecular Bonds in Scanning Tunneling Microscopy. *J. Am. Chem. Soc.* **2010**, *132*, 11864−11865.

(15) Tautz, R. T.; S. S; O. N; A. C. L; F. S. A Novel Method Achieving Ultra-High Geometrical Resolution in Scanning Tunnelling Microscopy. *New J. Phys.* **2008**, *10*, 53012.

(16) Li, S.; Yuan, D.; Yu, A.; Czap, G.; Wu, R.; Ho, W. Rotational Spectromicroscopy: Imaging the Orbital Interaction between Molecular Hydrogen and an Adsorbed Molecule. *Phys. Rev. Lett.* **2015**, *114*, 206101.

(17) Merino, P.; Rosławska, A.; Leon, C. C.; Grewal, A.; Große, C.; González, C.; Kuhnke, K.; Kern, K. A Single Hydrogen Molecule as an Intensity Chopper in an Electrically Driven Plasmonic Nanocavity. *Nano Lett.* **2019**, *19*, 235−241.

(18) Therrien, A. J.; Pronschinske, A.; Murphy, C. J.; Lewis, E. A.; Liriano, M. L.; Marcinkowski, M. D.; Sykes, E. C. H. Collective Effects in Physisorbed Molecular Hydrogen on Ni/Au(111). *Phys. Rev. B: Condens. Matter Mater. Phys.* **2015**, *92*, 161407.

(19) Yang, K.; Xiao, W.; Liu, L.; Fei, X.; Chen, H.; Du, S.; Gao, H.-J. Construction of Two-Dimensional Hydrogen Clusters on Au(111) Directed by Phthalocyanine Molecules. *Nano Res.* **2014**, *7*, 79−84.

(20) Corma, A.; Boronat, M.; Gonzalez, S.; Illas, F. On the Activation of Molecular Hydrogen by Gold: A Theoretical Approximation to the Nature of Potential Active Sites. *Chem. Commun.* **2007**, 3371−3373.

(21) Hammer, B.; Norskov, J. K. Why Gold Is the Noblest of All the Metals. *Nature* **1995**, *376*, 238−240.

(22) Zhang, Y.; Cui, X.; Shi, F.; Deng, Y. Nano-Gold Catalysis in Fine Chemical Synthesis. *Chem. Rev.* **2012**, *112*, 2467−2505.

(23) Takei, T.; Akita, T.; Nakamura, I.; Fujitani, T.; Okumura, M.; Okazaki, K.; Huang, J.; Ishida, T.; Haruta, M. Heterogeneous Catalysis by Gold. *Adv. Catal.* **2012**, *51*, 1−126.

(24) Jaramillo, T. F.; Baeck, S.-H.; Cuenya, B. R.; McFarland, E. W. Catalytic Activity of Supported Au Nanoparticles Deposited from Block Copolymer Micelles. *J. Am. Chem. Soc.* **2003**, *125*, 7148−7149.

(25) Fujitani, T.; Nakamura, I.; Akita, T.; Okumura, M.; Haruta, M. Hydrogen Dissociation by Gold Clusters. *Angew. Chem., Int. Ed.* **2009**, *48* (50), 9515−9518.

(26) Kartusch, C.; van Bokhoven, J. A. Hydrogenation over Gold Catalysts: The Interaction of Gold with Hydrogen. *Gold Bull.* **2009**, *42*, 343−348.

(27) Mukherjee, S.; Libisch, F.; Large, N.; Neumann, O.; Brown, L. V.; Cheng, J.; Lassiter, J. B.; Carter, E. A.; Nordlander, P.; Halas, N. J. Hot Electrons Do the Impossible: Plasmon-Induced Dissociation of H2 on Au. *Nano Lett.* **2013**, *13*, 240−247.

(28) Haruta, M. Spiers Memorial Lecture Role of Perimeter Interfaces in Catalysis by Gold Nanoparticles. *Faraday Discuss.* **2011**, *152*, 11−32.

(29) Jelínek, P.; Pérez, R.; Ortega, J.; Flores, F. Hydrogen Dissociation over Au Nanowires and the Fractional Conductance Quantum. *Phys. Rev. Lett.* **2006**, *96*, 46803.

(30) Zanchet, A.; Dorta-Urra, A.; Roncero, O.; Flores, F.; Tablero, C.; Paniagua, M.; Aguado, A. Mechanism of Molecular Hydrogen Dissociation on Gold Chains and Clusters as Model Prototypes of Nanostructures. *Phys. Chem. Chem. Phys.* **2009**, *11*, 10122−10131.

(31) Lock, D.; Rusimova, K. R.; Pan, T. L.; Palmer, R. E.; Sloan, P. A. Atomically Resolved Real-Space Imaging of Hot Electron Dynamics. *Nat. Commun.* **2015**, *6*, 8365.

(32) Schendel, V.; Borca, B.; Pentegov, I.; Michnowicz, T.; Kraft, U.; Klauk, H.; Wahl, P.; Schlickum, U.; Kern, K. Remotely Controlled Isomer Selective Molecular Switching. *Nano Lett.* **2016**, *16*, 93−97.

(33) Li, S.; Yu, A.; Toledo, F.; Han, Z.; Wang, H.; He, H. Y.; Wu, R.; Ho, W. Rotational and Vibrational Excitations of a Hydrogen Molecule Trapped within a Nanocavity of Tunable Dimension. *Phys. Rev. Lett.* **2013**, *111*, 146102.

(34) Wang, H.; Li, S.; He, H.; Yu, A.; Toledo, F.; Han, Z.; Ho, W.; Wu, R. Trapping and Characterization of a Single Hydrogen Molecule in a Continuously Tunable Nanocavity. *J. Phys. Chem. Lett.* **2015**, *6*, 3453−3457.

(35) Martínez, J. I.; Abad, E.; González, C.; Flores, F.; Ortega, J. Improvement of Scanning Tunneling Microscopy Resolution with H-Sensitized Tips. *Phys. Rev. Lett.* **2012**, *108*, 246102.

https://dx.doi.org/10.1021/acsnano.0c05507
ACS Nano XXXX, XXX, XXX−XXX

(36) Chiang, C.; Xu, C.; Han, Z.; Ho, W. Real-Space Imaging of Molecular Structure and Chemical Bonding by Single-Molecule Inelastic Tunneling Probe. *Science* **2014**, *344*, 885−888.
(37) de la Torre, B.; Švec, M.; Foti, G.; Krejčí, O.; Hapala, P.; Garcia-Lekue, A.; Frederiksen, T.; Zbořil, R.; Arnau, A.; Vázquez, H.; Jelinek, P. Submolecular Resolution by Variation of the Inelastic Electron Tunneling Spectroscopy Amplitude and Its Relation to the AFM/STM Signal. *Phys. Rev. Lett.* **2017**, *119*, 166001.
(38) Han, Z.; Czap, G.; Xu, C.; Chiang, C.; Yuan, D.; Wu, R.; Ho, W. Probing Intermolecular Coupled Vibrations between Two Molecules. *Phys. Rev. Lett.* **2017**, *118*, 36801.
(39) Czap, G.; Han, Z.; Wagner, P. J.; Ho, W. Detection and Characterization of Anharmonic Overtone Vibrations of Single Molecules on a Metal Surface. *Phys. Rev. Lett.* **2019**, *122*, 106801.
(40) Hanke, F.; Björk, J. Structure and Local Reactivity of the Au(111) Surface Reconstruction. *Phys. Rev. B: Condens. Matter Mater. Phys.* **2013**, *87*, 235422.
(41) Zanchet, A.; Roncero, O.; Dorta-Urra, A.; Aguado, A.; Martínez, J. I.; Flores, F.; Lorente, N. Electron Transport Signature of H2 Dissociation on Atomic Gold Wires. *Phys. Rev. B: Condens. Matter Mater. Phys.* **2014**, *90*, 41404.
(42) Smit, R. H. M.; Noat, Y.; Untiedt, C.; Lang, N. D.; van Hemert, M. C.; van Ruitenbeek, J. M. Measurement of the Conductance of a Hydrogen Molecule. *Nature* **2002**, *419*, 906−909.
(43) Horcas, I.; Fernandez, R.; Gomez-Rodriguez, J. M.; Colchero, J.; Gomez-Herrero, J.; Baro, A. M. WSXM: A Software for Scanning Probe Microscopy and a Tool for Nanotechnology. *Rev. Sci. Instrum.* **2007**, *78*, 13705.
(44) Lewis, J. P.; Jelínek, P.; Ortega, J.; Demkov, A. A.; Trabada, D. G.; Haycock, B.; Wang, H.; Adams, G.; Tomfohr, J. K.; Abad, E.; Wang, H.; Drabold, D. A. Advances and Applications in the FIREBALL *ab Initio* Tight-Binding Molecular-Dynamics Formalism. *Phys. Status Solidi B* **2011**, *248*, 1989−2007.
(45) González, C.; Abad, E.; Dappe, Y. J.; Cuevas, J. C. Theoretical Study of Carbon-Based Tips for Scanning Tunnelling Microscopy. *Nanotechnology* **2016**, *27*, 105201.

https://dx.doi.org/10.1021/acsnano.0c05507
ACS Nano XXXX, XXX, XXX−XXX